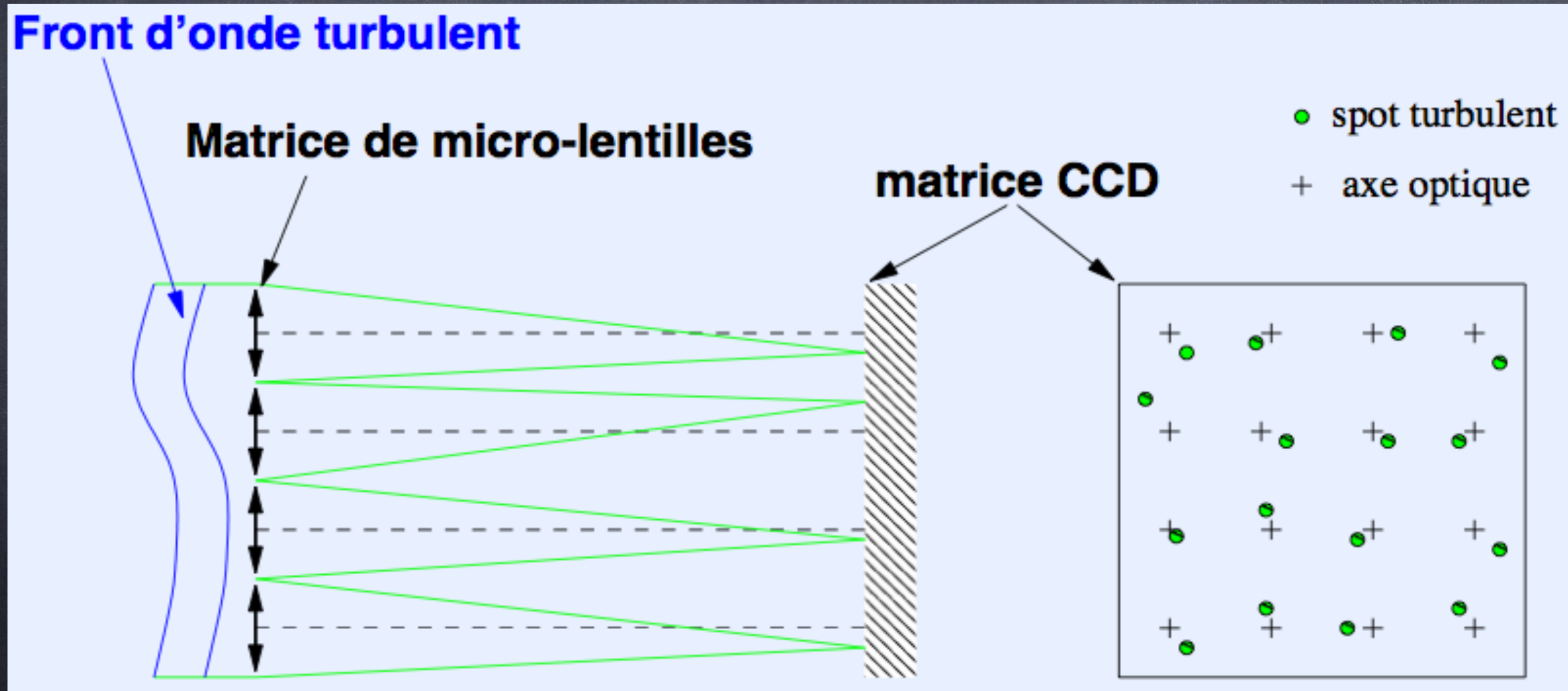


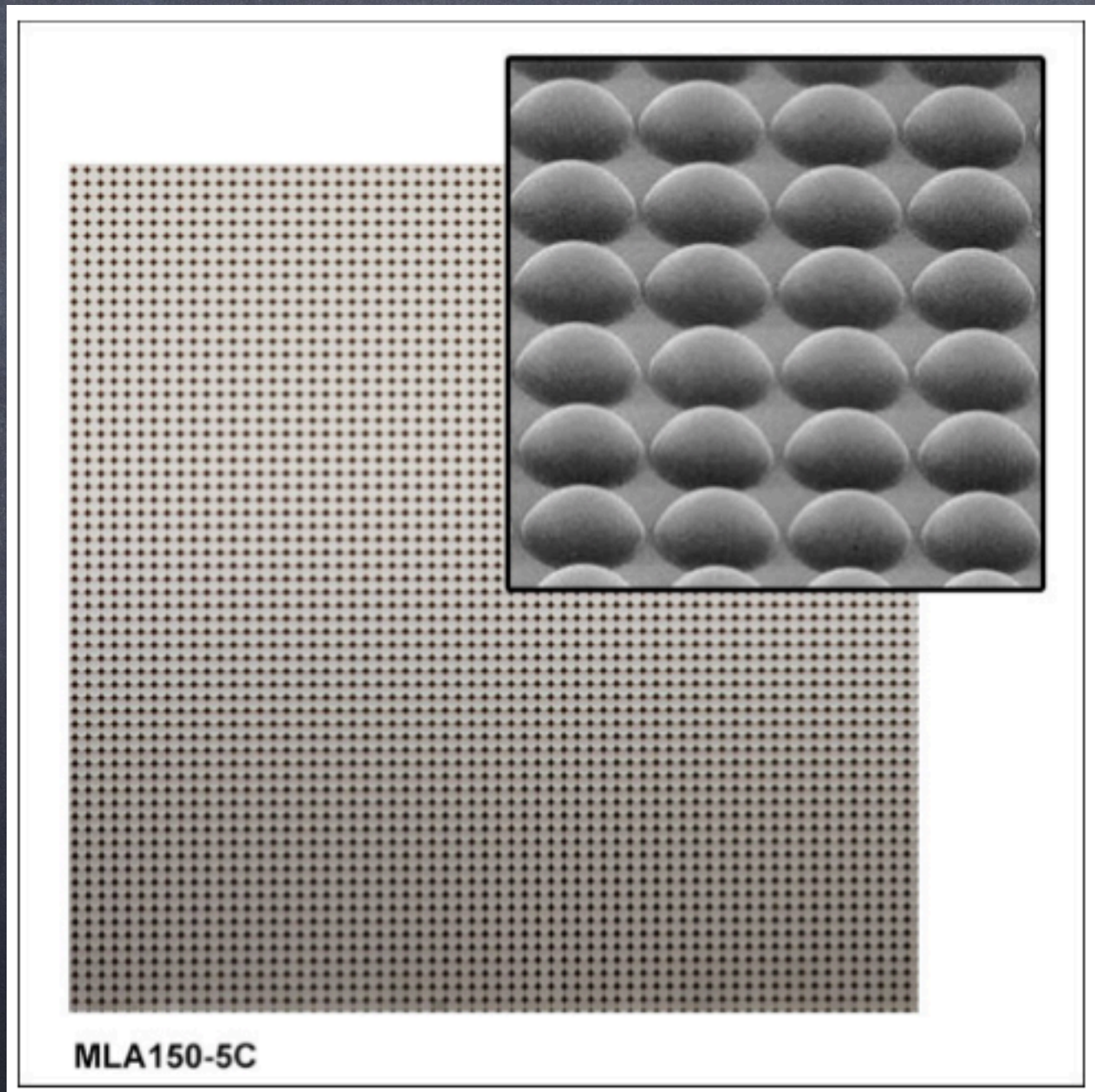
Wavefront sensors - 1

First example of wavefront sensor: Shack-Hartmann



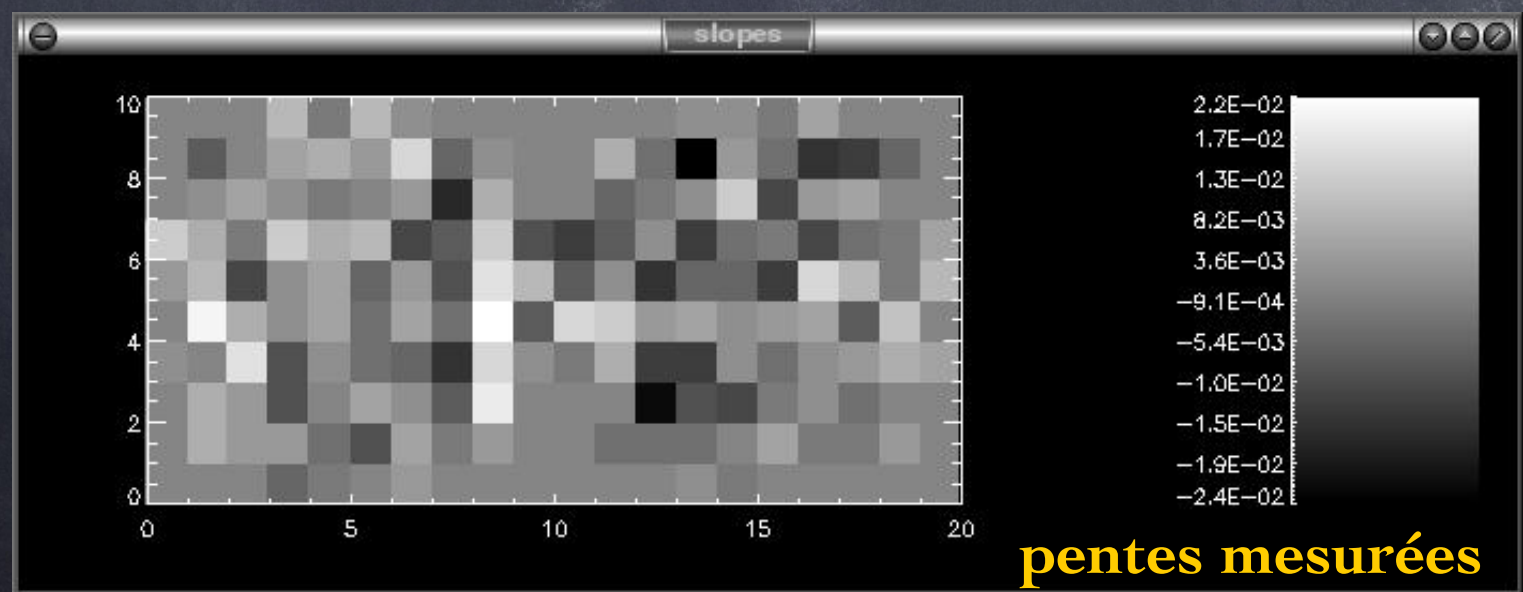
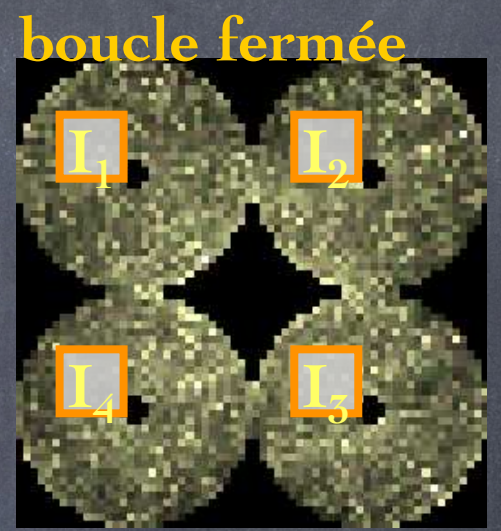
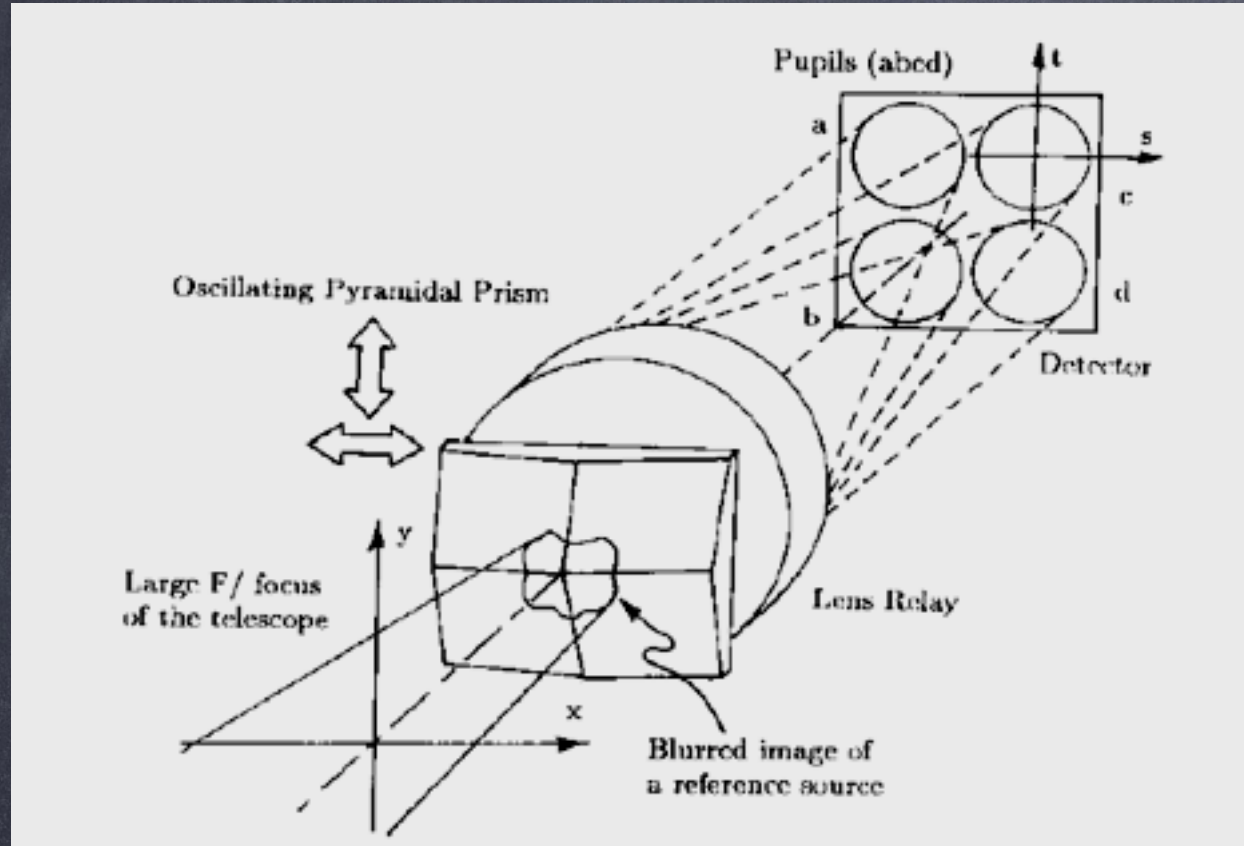
Wavefront sensors - 2

First example of wavefront sensor: Shack-Hartmann



Wavefront sensors - 3

Another example: the Pyramid WFS

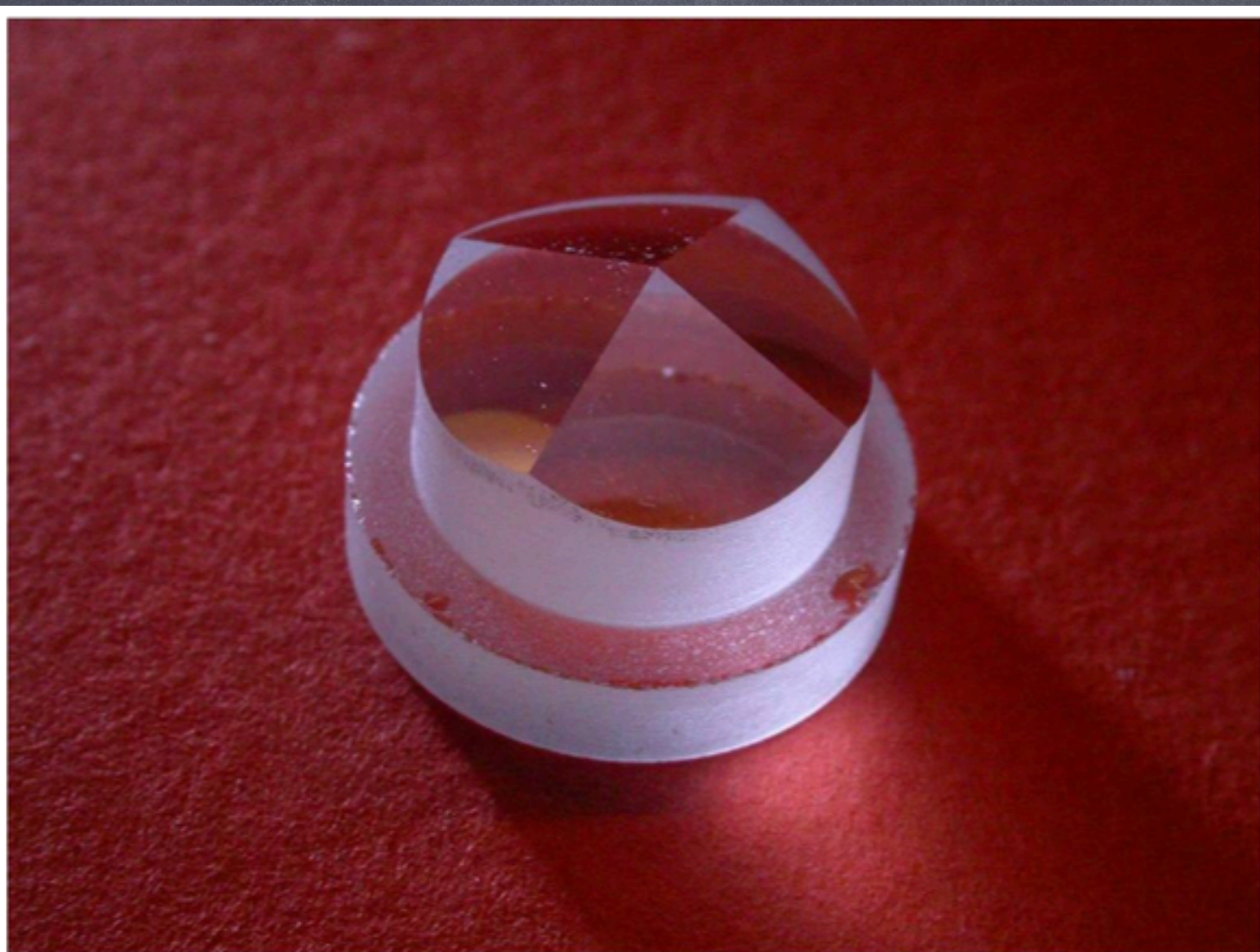


$$S_x(x, y) = \frac{(I_1 + I_4) - (I_2 + I_3)}{\sum_i I_i}$$

$$S_y(x, y) = \frac{(I_1 + I_2) - (I_3 + I_4)}{\sum_i I_i}$$

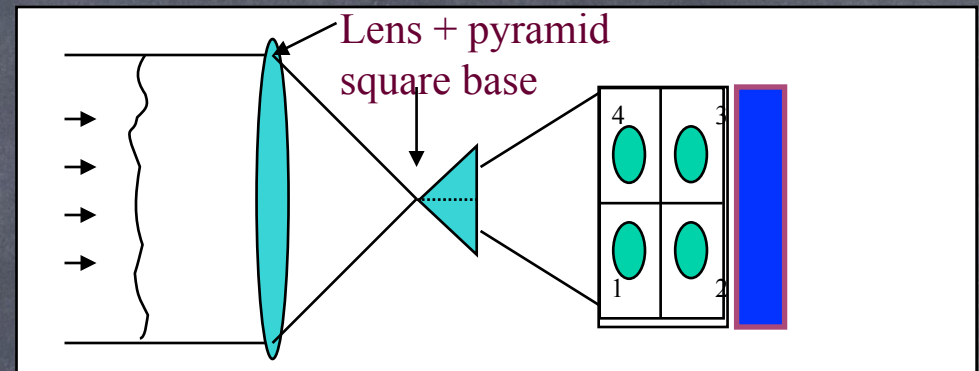
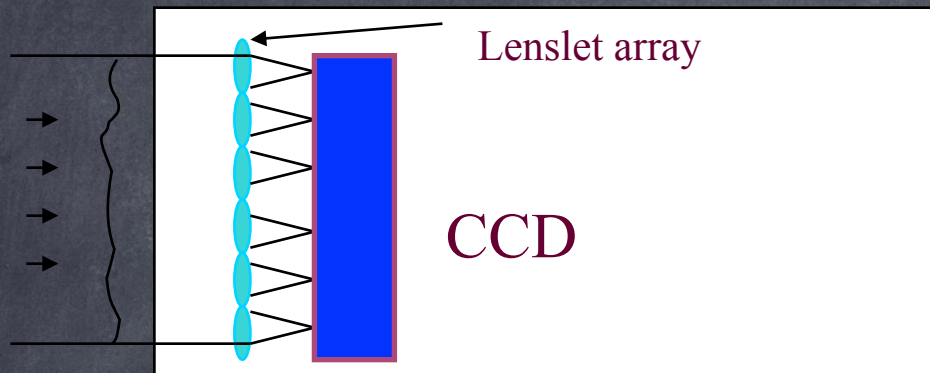
Wavefront sensors - 4

Another example: the Pyramid WFS



WH telescope's AO system

Wavefront sensors - 5



- SH: First on-sky AO results with COME-ON/VLT in 1989 [Rousset et al. 1990].
- Pyramid [Ragazzoni 1996], 2-mag. gain foreseen with respect to SH [Ragazzoni & Farinato 1999], confirmed by Monte-Carlo simulations [Esposito & Riccardi 2001].

Wavefront sensors - 6

Pyramid vs. Shack-Hartmann, 1st round

- Rousset et al., 1989-1990: 1st results of a SH WFS on sky on the VLT (COME-ON)
- Ragazzoni, 1996: proposal of a pyramid WFS
- Ragazzoni & Farinato, 1999: theoretical gain of 2 mag. (in limiting mag.)
- Esposito & Riccardi, 2001: gain confirmed by numerical simulations (but in open-loop and not the whole AO error budget)
- Carbillet et al., 2003: gain in limiting mag. confirmed (close loop & whole AO error), but also in the bright-end (lower aliasing!), from end-to-end simulations (for FLAO@LBT).

Wavefront sensors - 7

Pyramid vs. Shack-Hartmann, 2nd round

- Poyneer & Macintosh, 2004: spatial filtering of the SH WFS (lower aliasing error)
- Nicolle et al., 2004: optimized calculus of the SH signals (lower measurement error)
- Fusco et al., 2005: spatial filtering+optimized calculus => SH at the level of the Pyramid (and less uncertainties on stability and robustness...)
- Vérinaud et al., 2005 (in the framework of XAO and the ELT): Pyramid better close to optical axis, SH ‘à la Fusco’ better far from it.

Wavefront sensors - 8

Pyramid vs. Shack-Hartmann, 2nd round

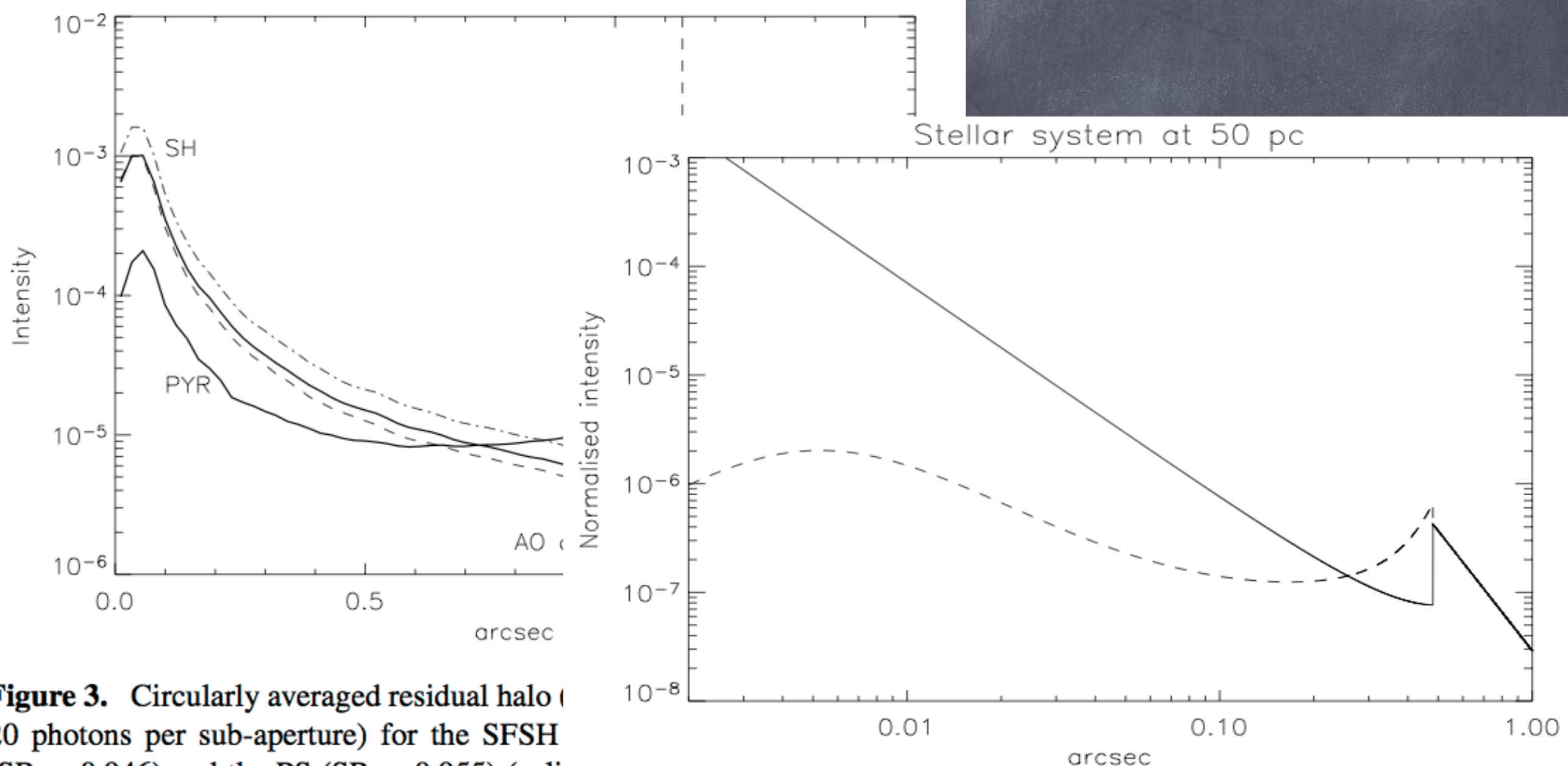


Figure 3. Circularly averaged residual halo (20 photons per sub-aperture) for the SFSH ($SR = 0.946$) and the PS ($SR = 0.955$) (solid line), the WCOG, 20 photons per sub-aperture (dot-dash line) and the AO (dashed line).

Figure 7. Residual halo in the *R* band for a SFSH-based system (solid line, $SR = 0.79$) and a PS-based system (dashed line, $SR = 0.81$) with a 15-cm actuator pitch on a 100-m telescope. The guide star *V* magnitude is 8.2, seeing = 0.7 arcsec, $\tau_0 = 3$ ms, frame rate = 4 kHz.

Wavefront sensors - 9

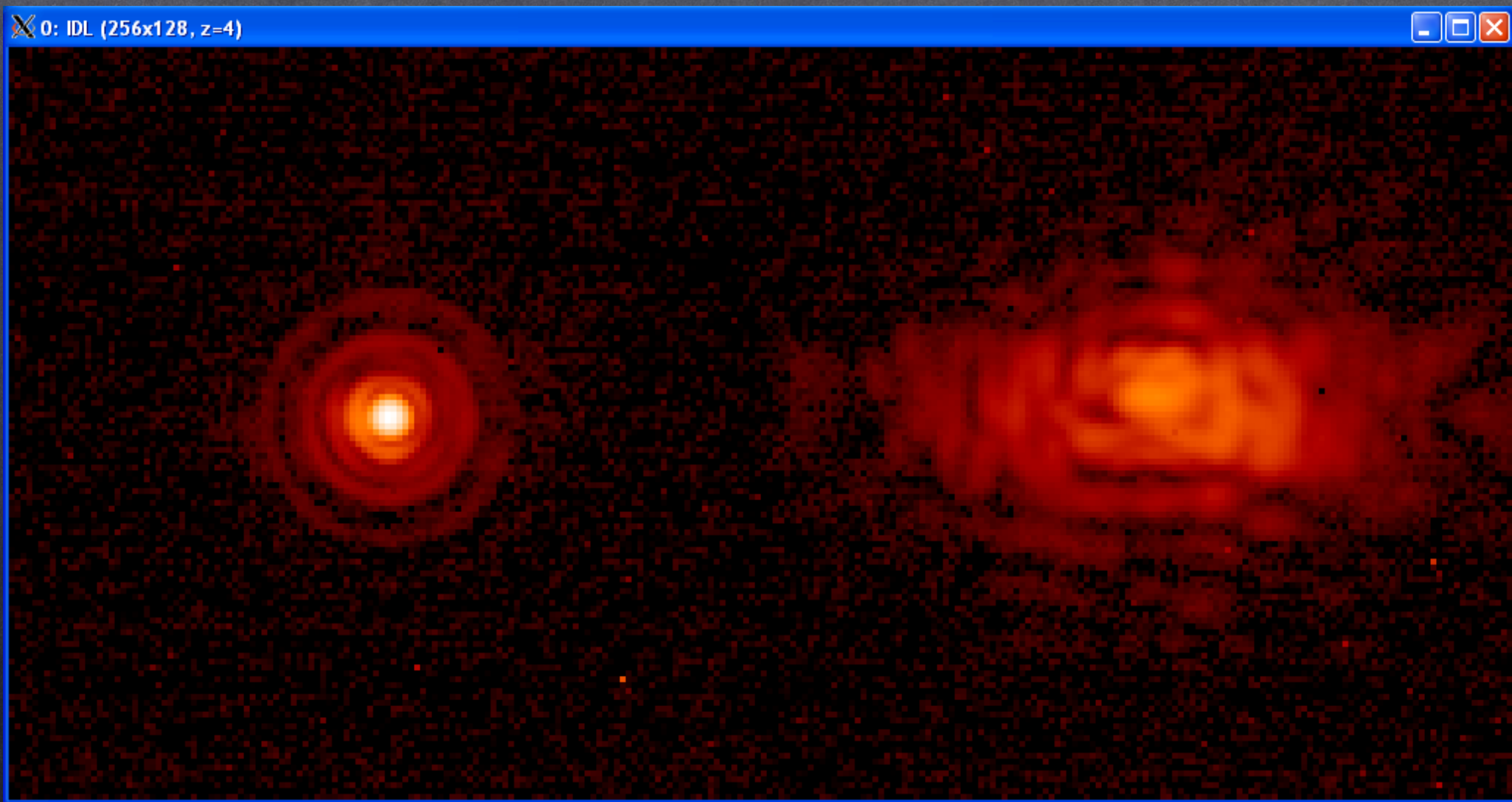
Pyramid vs. Shack-Hartmann, 3rd round

Press release (may/june 2010): LBT achieves breakthrough with adaptive optics ! (<http://oldweb.lbto.org/AO/AOpressrelease.htm>)

Wavefront sensors - 10

Pyramid vs. Shack-Hartmann, 4th round

(2014)



Deformable correctors - 1

- Different technologies for correctors:
 - piezo-stacked arrays
 - piezo-electric bimorph mirrors
 - MEMS
 - voice-coil adaptive secondary mirrors (ASM)
 - multi-actuator adaptive lens (MAL) (!)
- Different coefficients for the fitting error, different strokes, different possible bandwidths, different possible number of modes, possible hysteresis, etc.

Deformable correctors - 2

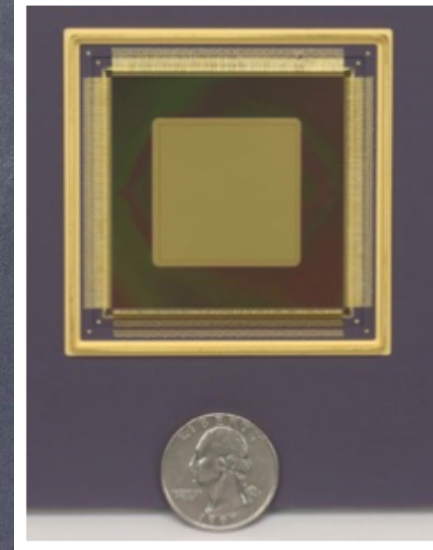
146mm clear aperture



349 actuators on 7 mm spacing



@Boston MC



MEMS

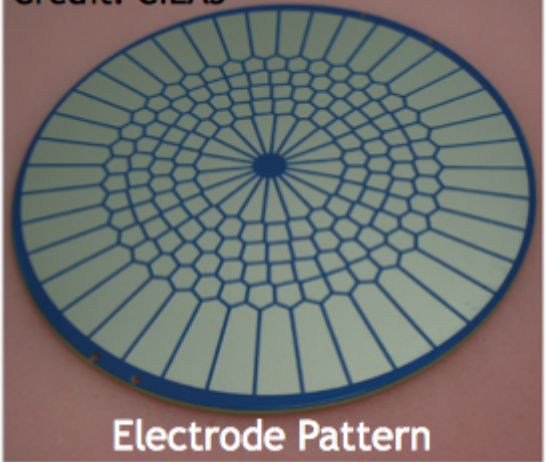
Voice-coil
('adaptive secondary')

Kinetics @ Keck

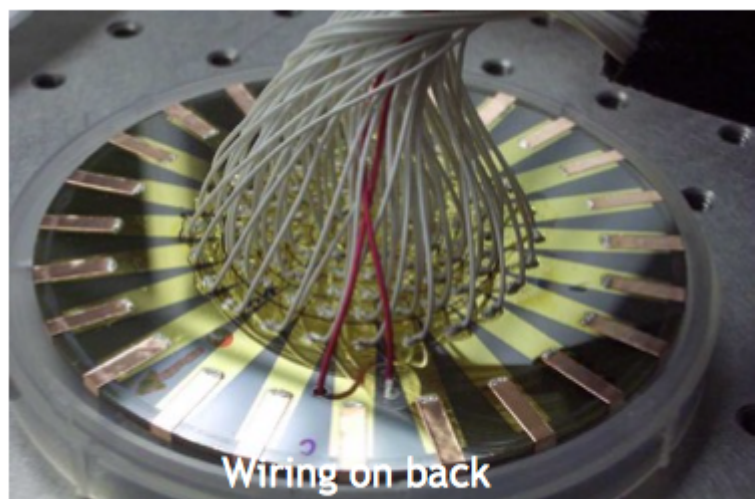
Piezo-stacked array

Bimorph

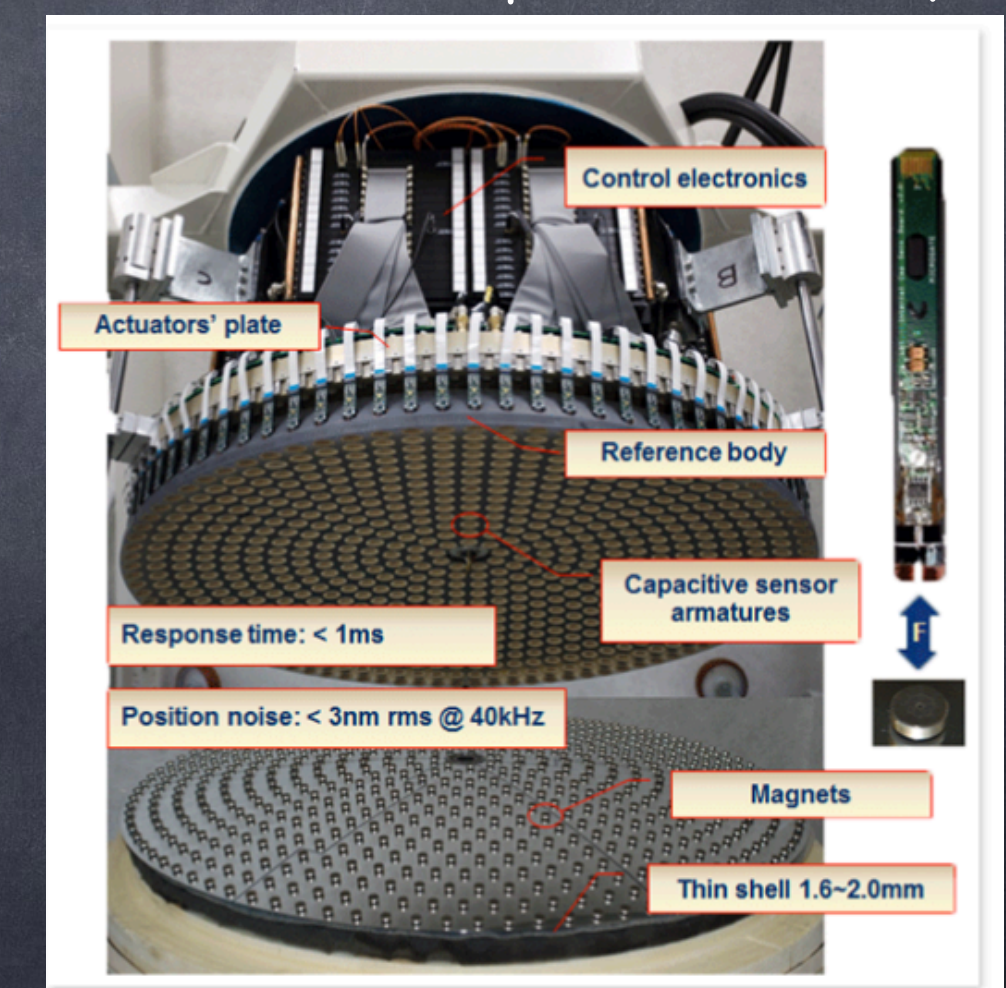
Credit: CILAS



Electrode Pattern



Wiring on back



(c) Micro gate

Deformable correctors - 3

- Different coefficients for the fitting error:



- Is the stroke enough ?
If not: necessity to add a tip-tilt mirror...

Deformable correctors - 4

- How many actuators for a given Strehl ratio ?
(considering a coeff. 0.3 for the fitting error)

$$\sigma_{\text{fit.}}^2 = 0.3 \left(\frac{d_{\text{act.}}}{r_0} \right)^{\frac{5}{3}}$$

$$S_{\max} = \exp(-\sigma_{\text{fit.}}^2)$$

- if $d = r_0$, then: $S_{\max} = \exp(-0.3) \approx 0.74$
if $d = r_0/2$, then: $S_{\max} = \exp(-0.3/2^{5/3}) \approx 0.91$

Deformable correctors - 5

- Influence functions → mirror modes

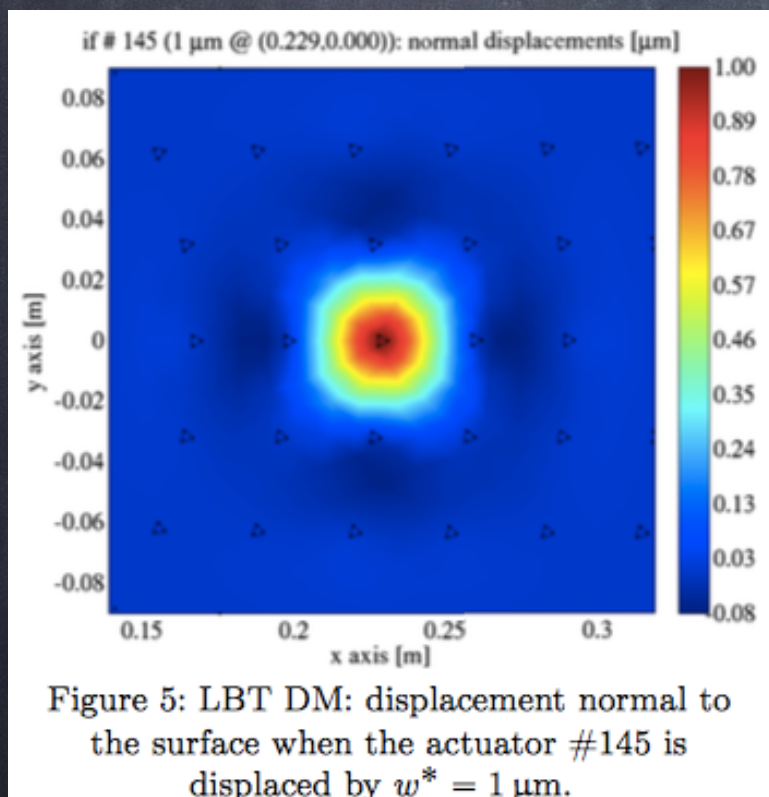
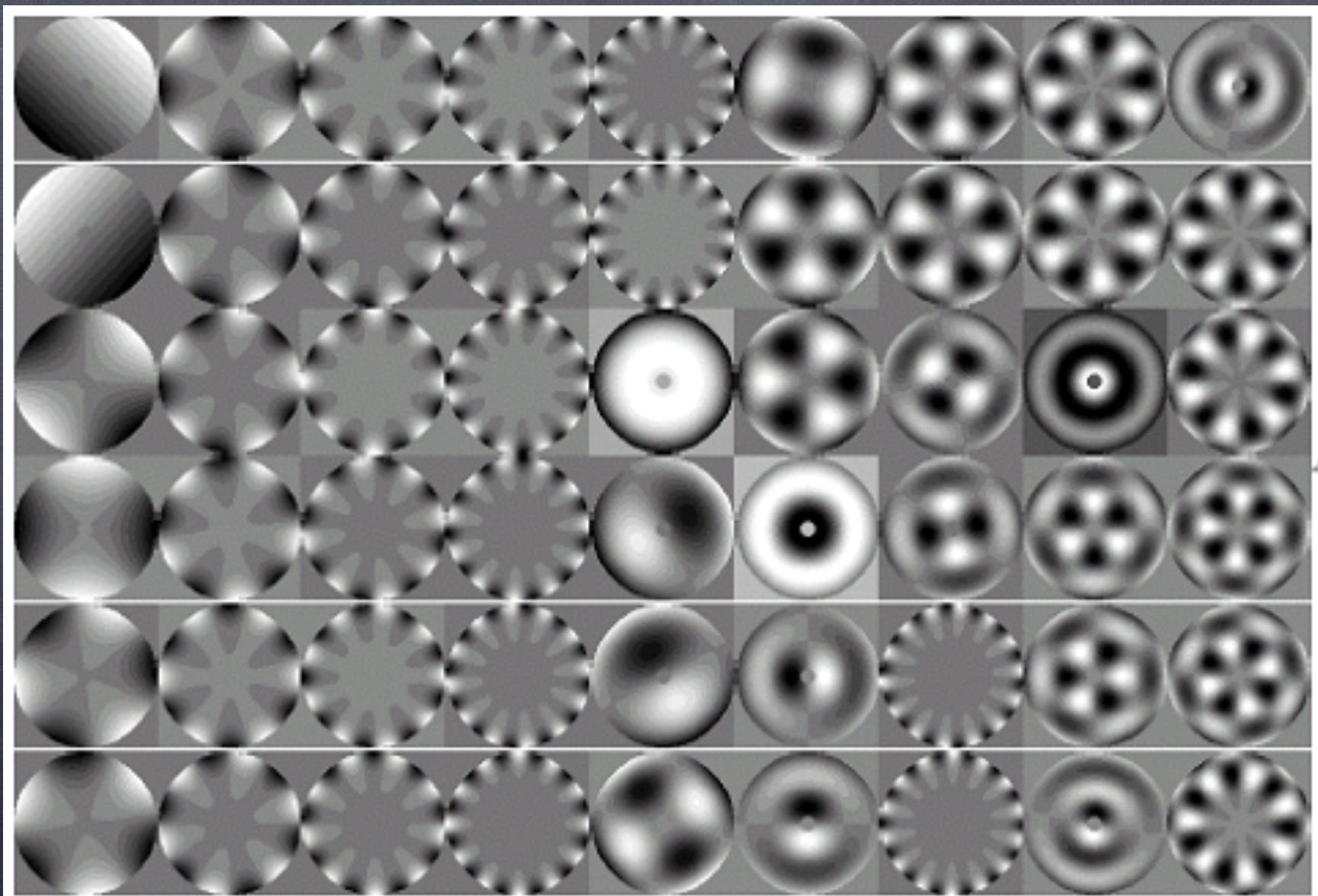
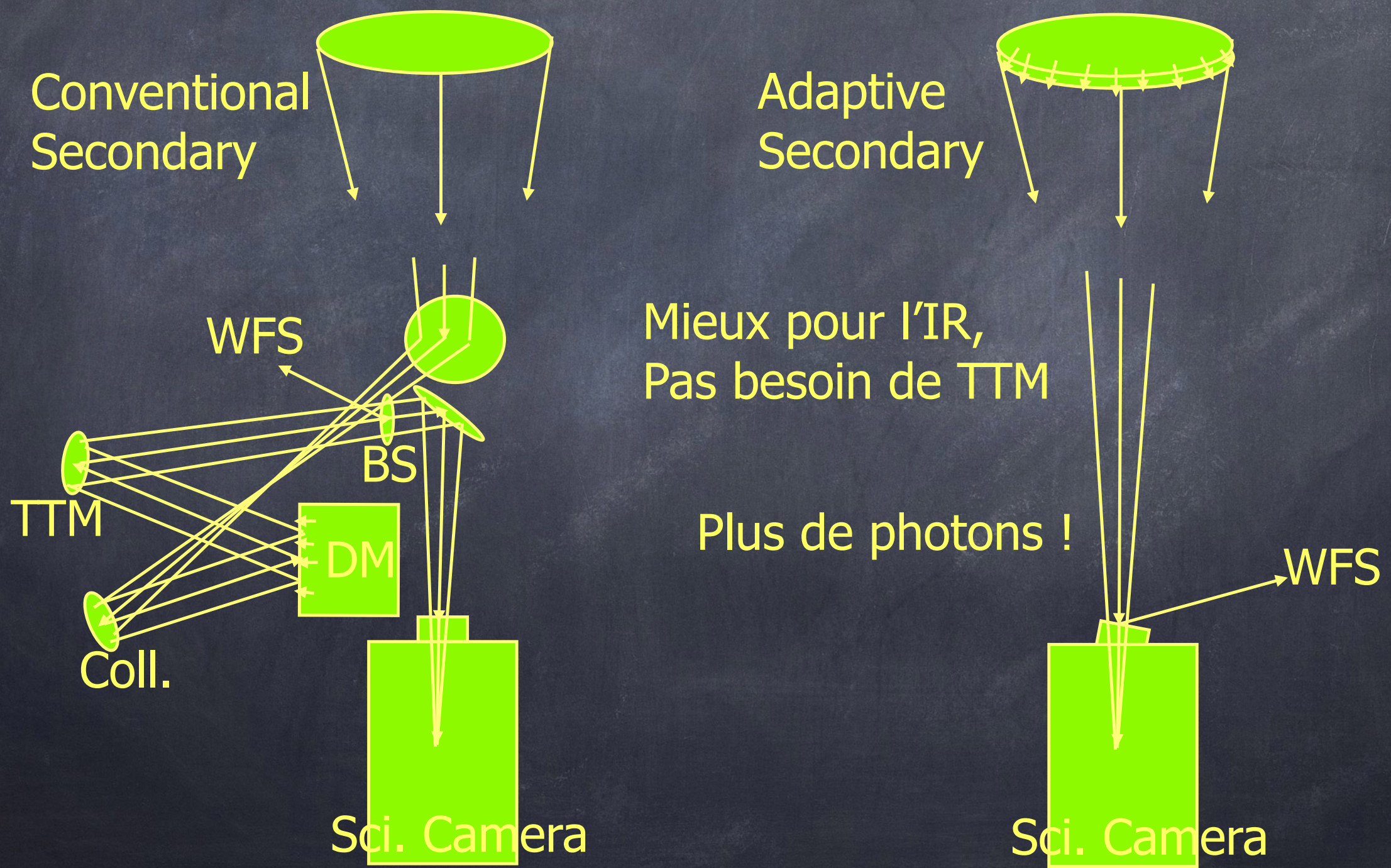


Figure 5: LBT DM: displacement normal to the surface when the actuator #145 is displaced by $w^* = 1 \mu\text{m}$.



Deformable correctors - 6

- An interesting case: the Adaptive Secondary Mirror (ASM) technology developed for LBT [Brusa et al. 2003]



Reconstruction & control of the commands - 1

Pure integrator case:

$$c_{t+1} = c_t + g A m_t$$

where c is the commands vector (n actuators), m the measurement vector (m elements), g a scalar loop gain ($0 < g < 1$), A the ($n \times m$) command matrix.

The commands matrix A is, in practice, the pseudo-inverse (SVD) of the measured (during calibration stage) interaction matrix D ($m \times n$):

$$A = D^+ = V \Sigma^+ U^*$$

where Σ is an $m \times n$ rectangular diagonal matrix with non-negative numbers on the diagonal (Σ_{ii} are the singular values of D), and U ($m \times m$) and V ($n \times n$) are orthonormal unitary matrices. (Note : $D^+ = (D^t D)^{-1} D^t$)

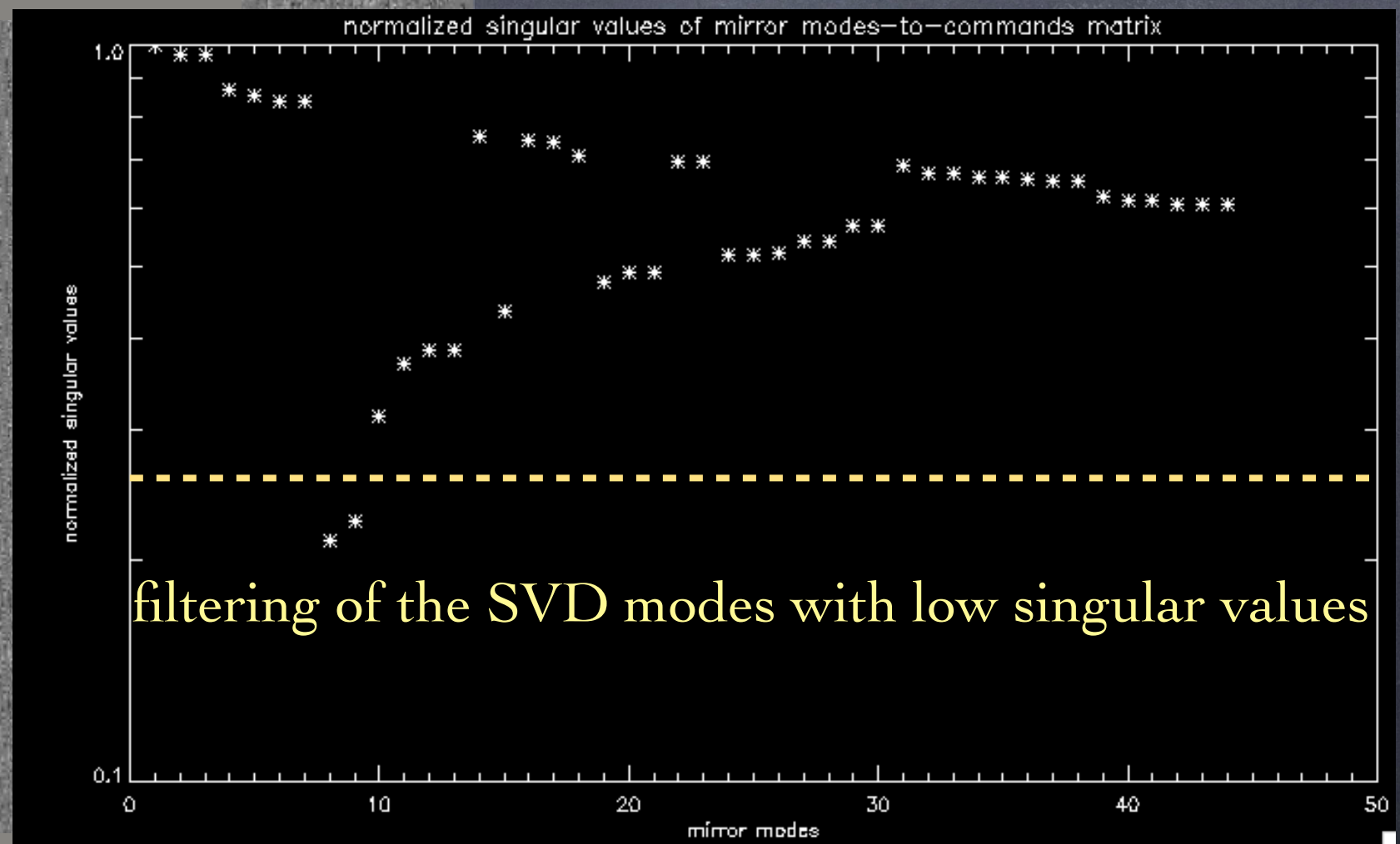
Filtering of SVD modes: Σ_{ii} ‘too small’ $\Rightarrow \Sigma^+_{ii}$ set to 0 (truncated SVD).

Reconstruction & control of the commands - 2

interaction matrix

m mirror modes

n slope measurements (x & y)



Reconstruction & control of the commands - 3

Reconstruction	Contrôle
Inverse généralisée (SVD tronquée) → matrice d'interaction	Intégrateur (ou autre filtrage temp.) → déf. du filtre, déf. des gains/mode
MAP (Fusco 2001) → + coeff. bruit, var./covar. spat.	Idem
OMGI (Gendron & Léna 1994) → matrice d'int., coeff. bruit/mode, DS de la phase/mode (débruitée)	
OMGI alternatif (Dessenes 1998) → matrice d'int., DS de la phase/mode (bruitée)... + ajustement de la DS !	
Kalman (éq. MAP en boucle fermée - Le Roux et al. 2004) → matrice d'interaction, coeff. bruit, var./covar. spatio-temp.	

